

Efficient deep blue electrophosphorescent devices based on platinum(II) bis(*n*-methyl-imidazolyl)benzene chloride

Tyler Fleetham, Zixing Wang, Jian Li*

Materials Engineering, Arizona State University, Tempe, AZ 85284, United States

ARTICLE INFO

Article history:

Received 3 February 2012

Received in revised form 20 March 2012

Accepted 24 March 2012

Available online 17 April 2012

Keywords:

Blue OLED

Platinum complex

Phosphorescent emitter

ABSTRACT

Highly efficient deep blue phosphorescent light emitting diodes were developed using a newly synthesized series of blue emitting tridentate platinum emitters. Devices employing a cohort of hole and electron transport materials yielded high external quantum efficiencies with low turn on voltage and low efficiency roll off. A maximum EQE of 15.7% and CIE coordinates of (0.16,0.13) was achieved in a device based on platinum(II) bis(*N*-methyl-imidazolyl)benzene chloride (Pt-16).

© 2012 Elsevier B.V. All rights reserved.

1. Introduction

Organic light emitting diodes (OLEDs) have garnered great attention in recent decades as the next generation in flat panel and handheld displays for their benefits of potentially low energy consumption and high quality of color displays [1]. Phosphorescent Ir and Pt complexes are of particular interest due to their potential to harvest both electrogenerated singlet and triplet excitons and realize 100% internal quantum efficiency [2]. In order to cover the full visible spectrum, efficient and stable blue, green and red phosphorescent OLEDs will be needed. However, compared to their analogs emitting in the “green” and “red” region, efficient and stable blue phosphorescent materials remain a challenge [3–5]. So far, the approaches to achieve efficient blue-phosphorescent OLEDs are heavily focused on Ir-based complexes, with either adopting high triplet energy ligands like 4,6 difluorophenylpyridine [4a–e] and 1-phenyl-3-methylimidazolium [4f], or using electron-withdrawing ancillary ligands such as picolinate (FlrPic) [4a], tetrakis(1-pyrazolyl)borate (Flr6) [4b,c], triazole (Flrtaz) and tetrazolate (FlrN4) [4d]. Moreover, the phosphorescent emitters which enable an efficient deep

blue OLED with desirable CIE coordinates (0.15,0.15) are even more scarce [6,7]. So far, the best deep blue PhOLED, based on the literature report, has demonstrated a maximum forward viewing external quantum efficiency (EQE) of 24.2% and achieved CIE coordinates of (0.14,0.20), which employed iridium(III) bis(3',5'-difluoro-4'-cyanophenylpyridinato-N,C^{2'}) picolinate (FCNIrpic) as an emissive material [7a]. In another notable report, a maximum EQE of 18.6% was achieved with CIE coordinates of (0.15,0.19) for a device employing halogen-free *mer*-tris(*N*-dibenzofuranyl-*N'*-methylimidazole) iridium(III) [Ir(dbfmi)] as an emitter [6a]. Although the performance and color quality of deep blue phosphorescent OLEDs are satisfactory, the development of deep blue OLEDs with a long operational lifetime remains as a significant challenge. It is highly desirable that different classes of deep blue phosphorescent emitters be developed and studied for OLED applications.

Cyclometalated Pt complexes should also be considered as candidate materials for efficient deep blue OLEDs to further compliment this progress made with the class of Ir complexes. However, the photophysical properties of Pt complexes are very sensitive to the structural changes of the complexes or the selection of the metal complex system. For example, Pt(N[^]C[^]N)Cl complexes have demonstrated higher emission efficiencies and

* Corresponding author.

E-mail address: jian.li.1@asu.edu (J. Li).

shorter luminescent lifetimes than their (C^{^N})Pt(acac) and Pt(N^{^C}^{^N})Cl analogs, where N^{^C}^{^N} are tridentate coordinating ligands like di(2-pyridinyl)benzene, C^{^N} are bidentate coordinating ligands like phenylpyridine, and N^{^N}^{^C} are tridentate coordinating ligands like 2-phenylbipyridine [8]. Thus, efficient blue phosphorescent OLEDs can be fabricated utilizing the analogs of platinum(II) 3,5-di(2-pyridinyl)benzene chloride (Pt-1). Similar to the reported color tuning strategy on the (C^{^N})Pt(acac) complexes [5a], the maximum emission wavelength (λ_{max}) of Pt-1 analogs can be shifted to the shorter wavelength range by either stabilizing the highest occupied molecular orbital (HOMO) through the fluorination of the phenyl ring as in platinum(II) 1-fluoro-2,4-di(2-pyridinyl)benzene chloride (Pt-3) and platinum(II) 1,3-difluoro-4,6-di(2-pyridinyl)benzene chloride (Pt-4) (Fig. 1), or destabilizing the lowest unoccupied molecular orbital (LUMO) through the utilization of the electron accepting groups with higher reduction potential. Previously, we have demonstrated an efficient blue phosphorescent OLED based on Pt-4 with a maximum EQE of 16%, yet the CIE coordinates (0.16,0.26) are still unsatisfactory for a deep blue OLED [9]. Here we will attempt to replace pyridinyl groups of Pt-1 with methyl-imidazolyl groups or pyrazolyl groups, which could potentially increase the LUMO energy level of Pt complexes, resulting in blue-shifted emission spectra. Although deep blue Ir-based emitters like Ir(dbfmi) utilize the ligands of phenyl-3-methylimidazolium and its analogs [6a], (C^{^N})Pt(acac) complexes incorporated with such ligands did not appear to have comparable device performance to their Ir analogs [10]. Moreover, the development of Pt(N^{^C}^{^N})Cl analogs employing such cyclometalating ligands required much more synthetic efforts than that of their Ir analogs. In this communication, we report the synthesis, photophysics and device characterization of a series of blue-emitting Pt complexes employing such cyclometalating ligands. One of our developed Pt complexes, i.e. platinum(II) bis(N-methylimidazolyl)benzene chloride (Pt-16) shown in Fig. 1, enabled us to fabricate an efficient deep blue phosphorescent OLED with a maximum EQE of 15.7% and CIE coordinates of (0.16,0.13).

2. Experimental

2.1. Materials

Poly [3,4-ethylenedioxythiophene] doped with poly[styrene sulfonate] (PEDOT:PSS, Clevis P VP Al 4083) was purchased from Stark Inc. and 2,9-dimethyl-4,7-diphenyl-1,10-phenanthroline (BCP) and N,N'-diphenyl-N,N'-bis(1-naphthyl)-1,1'-biphenyl-4,4''-diamine (NPD) were purchased from Aldrich and sublimed in a thermal gradient furnace prior to use. 2,8-bis(diphenyl phosphoryl) dibenzothiophene (PO15), [12] di-[4-(N,N-di-tolyl-amino)-phenyl]cyclohexane (TAPC) [12], 2,6-bis(N-carbazolyl)pyridine (26mCPy) [11a] and platinum 1,3-difluoro-4,6-di(2-pyridinyl)benzene chloride (Pt-4) [8] were prepared following literature procedure.

2.2. Synthesis

A series of blue-emitting Pt complexes were designed and synthesized following the strategy presented in Fig. 1, which include platinum(II) bis(C-methyl-imidazolyl)benzene chloride (Pt-14), platinum(II) bis(3,5-dimethyl-pyrazolyl)benzene chloride (Pt-15) and Pt-16.

2.2.1. Synthesis of Pt-14

A mixture of *m*-di(methyl-imidazolyl)benzene (1 mmol), K₂PtCl₄ (0.41 g, 1 mmol), and acetic acid (60 mL) was stirred under reflux for 3 days in nitrogen atmosphere. After cooling to room temperature, the reaction mixture was filtered. The precipitate was washed with methanol, water, ethanol and ether. The light yellowish product (in 50% yield) was obtained after thermal evaporation under high vacuum. ¹H NMR (400 MHz, CDCl₃): 7.40 (dd, 2H), 7.28 (d, 2H), 7.13 (t, 1H), 6.93 (d, 2H), 3.98 (s, 6H). HRMS (MALDI-TOF) *m/z* for [(M+H)⁺] calcd. 468.056, found 468.080.

2.2.2. Synthesis of Pt-15

A mixture of K₂PtCl₄, *m*-bis(3,5-dimethyl-pyrazolyl)benzene (1 mmol) and 3 mL of AcOH/H₂O (9:1, v/v)

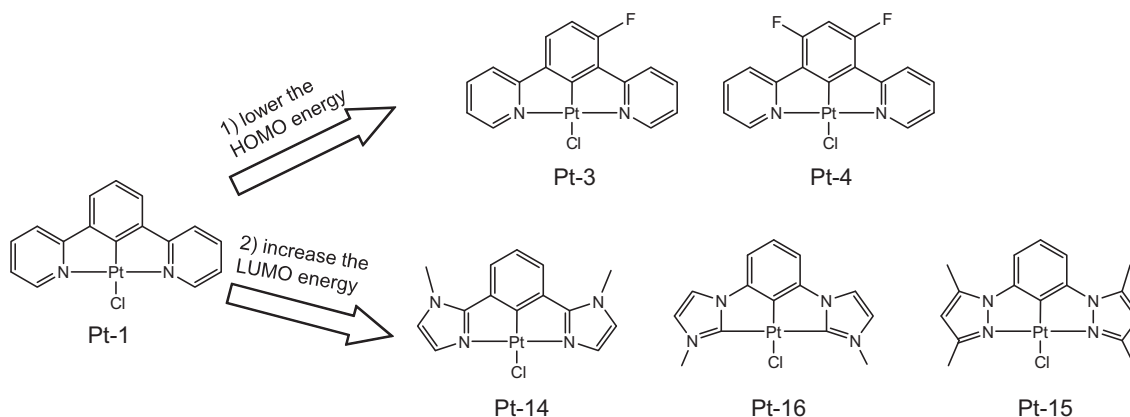


Fig. 1. Materials design and chemical structures of tridentate platinum-based blue phosphorescent emitters discussed in this paper.

was placed in a 10 mL Pyrex pressure vessel. The tube was capped and rapidly heated by the microwave reactor (2450 MHz, 200 W). The reaction mixture was kept at 160 °C for 30 min by controlling the flow rate of cooling air. After cooling to room temperature, the reaction mixture was filtered. The precipitate was washed with methanol, water, ethanol and ether. The crude product was further purified by train sublimation with a 70% yield. ^1H NMR (400 MHz, CDCl_3): 7.17–7.26 (m, 3H), 6.31 (s, 2H), 2.71 (s, 3H), 2.61 (s, 3H). HRMS (MALDI-TOF) m/z for $[(M + H)^+]$ calcd. 496.087, found 496.101.

2.2.3. Synthesis of Pt-16

A mixture of bis(N-methyl-imidazolium)benzene diiodide (1 mmol) and 0.5 mmol silver oxide was stirred in a solution of 100 ml acetonitrile for 5 h at room temperature before 1 equiv. platinum chloride and 1 equiv. potassium carbonate were added. The reaction mixture was heated to reflux for additional 24 h. Then the mixture was cooled to room temperature before 100 ml water was added. The resulting yellow precipitate was filtered off and washed with excessive methanol, water and ether and dried under vacuum. The light yellowish product (in 4% yield) was obtained after thermal evaporation under high vacuum. ^1H NMR (400 MHz, CDCl_3): δ 7.35 (d, 2H), 7.180 (dd, 1H), 6.90–6.96 (m, 4H), 4.37(s, 6H). HRMS (MALDI-TOF) m/z for $[(M + H)^+]$ calcd. 468.056, found 468.082.

2.3. Materials characterization

Steady-state emission experiments at room temperature were performed on a Jobin Yvon Fluorolog spectrofluorometer. Cyclic voltammetry and differential pulsed voltammetry were performed using a CHI610B electrochemical analyzer. Anhydrous DMF (Aldrich) was used as the solvent under a nitrogen atmosphere, and 0.1 M tetra(n-butyl) ammonium hexafluorophosphate was used as the supporting electrolyte. A silver wire was used as the pseudo reference electrode, a Pt wire was used as the counter electrode, and glassy carbon was used as the working electrode. The redox potentials are based on the values measured from differential pulsed voltammetry and are reported relative to a ferrocene/ferrocenium (Fc/Fc^+) redox couple used as an internal reference. The reversibility of reduction or oxidation was determined using cyclic voltammetry.

2.4. Device fabrication and characterization

Devices employing Pt-4, Pt-14, Pt-15 and Pt-16 as emitters were fabricated on glass substrates pre-coated with a patterned transparent indium tin oxide (ITO) anode using a general structure of ITO/PEDOT:PSS/NPD(30 nm)/TAPC(10 nm)/2% emitter:26mCPy(25 nm)/PO15(40 nm)/LiF/Al. Prior to organic depositions, the ITO substrates were cleaned by sonication in water, acetone, and isopropanol followed by UV-ozone treatment for 15 min. PEDOT:PSS was filtered through a 0.2 μm filter and spin-coated on the pre-cleaned substrates, giving a 40 nm thick film. Organic materials were thermally evaporated at deposition rates of 0.5–1.5 $\text{\AA}/\text{s}$ at a working pressure of less than

10^{-7} Torr. The deposition rates and thicknesses were monitored by quartz crystal microbalances. A thin 1 nm LiF layer was deposited at rates of $<0.2 \text{\AA}/\text{s}$. Aluminum cathodes were deposited at rates of 1–2 $\text{\AA}/\text{s}$ through a shadow mask without breaking vacuum. Individual devices had areas of 0.04 cm^2 . All device operation and measurement were carried out inside a nitrogen-filled glove-box. I – V – L characteristics were taken with a Keithley 2400 Source-Meter and a Newport 818 Si photodiode. EL spectra were taken using the Jobin Yvon Fluorolog spectrofluorometer. Agreement between luminance, optical power and EL spectra was verified with a calibrated Photo Research PR-670 Spectroradiometer with all devices assumed to be Lambertian emitters.

3. Results and discussion

The electrochemical properties of Pt-14, Pt-15, and Pt-16 were examined using cyclic voltammetry. Compared with Pt-1, the changes of the electron-accepting groups modify the reduction potential of the Pt complexes and leave the oxidation potential largely unaffected. Thus, the reduction potentials of these three Pt complexes are in the range between -2.7 and -2.8 V vs. Fc/Fc^+ , which are much higher than that of Pt-1 (Fig. 2 inset). The comparison of room temperature emission spectra of Pt-1, Pt-14, Pt-15 and Pt-16 is presented in Fig. 2, which were taken from the samples in a dilute solution of dichloromethane for Pt-1, Pt-14 and Pt-16, and a doped thin film sample for Pt-15. Although all three synthesized Pt complexes have similar oxidation and reduction potentials, their emission energies are significantly different. The λ_{max} values of Pt-14, Pt-16 and Pt-15 are 470, 448 and 430 nm, respectively. Both Pt-14 and Pt-16 emit strongly in a degassed solution at the room temperature, making them suitable as emitters for blue phosphorescent OLEDs. On the other hand, Pt-15 was weakly emissive in degassed solution and only provided a measurable photoluminescent spectrum in a 2%-doped PMMA film (Fig. 2). For Pt-15, the poor quantum

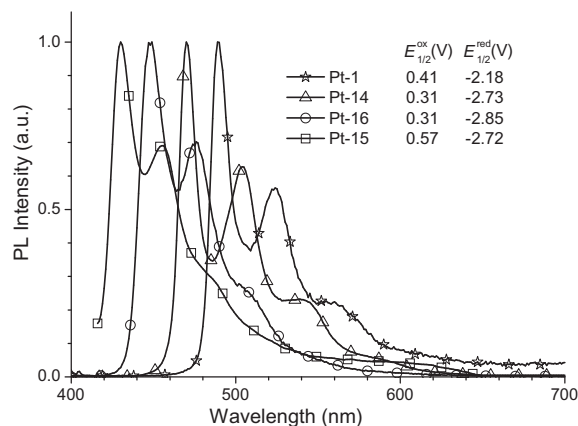


Fig. 2. Room temperature emission spectra of Pt-1 (stars), Pt-14 (triangles) and Pt-16 (circles) in CH_2Cl_2 and Pt-15 (squares) in a 2%-doped PMMA film. Redox values (V) are shown in the inset, which are reported relative to Fc/Fc^+ .

yield of emission can be attributed to a combined result of an accelerated high non-radiative decay rate and a low radiative decay rate, similar to its reported analogs like *fac*-Ir(ppz)₃ and Pt(dpzt)Cl [11].

The EQE values are plotted vs. current density for devices employing Pt-4, Pt-14, Pt-15 and Pt-16, in Fig. 3, with the corresponding EL spectra and CIE coordinates displayed in Fig. 4. A summary of device performance is presented in Table 1. The dopant concentration is controlled to

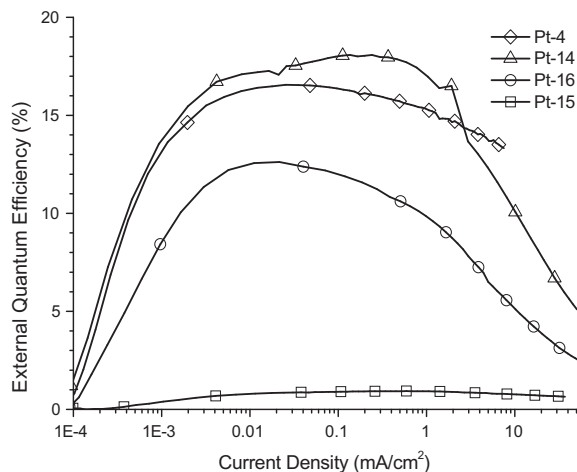


Fig. 3. External quantum efficiency–current density characteristics for Pt-4 (diamonds), Pt-14 (triangles), Pt-16 (circles) and Pt-15 (squares) devices with the structure of ITO/PEDOT:PSS/NPD(30 nm)/TAPC(10 nm)/2% emitter:26mCPy(25 nm)/PO15(40 nm)/LiF/Al.

be around 2%(w/w) to minimize the formation of excimers which tend to broaden the EL spectrum of device and increase the values of CIE coordinates [12].

Due to the use of a better hole blocking layer (PO15) and electron blocking layer (TAPC) than those reported in a previous Pt-4 device, the Pt-4 device has demonstrated an improved device efficiency (close to 17%) with a similar EL spectrum. This improvement indicates a good confinement of dopant excitons inside of emissive layer, and affirms that the triplet energy of host material (26mCPy) is suitable for the emitters [13]. Similarly, both Pt-14 and Pt-16 devices have demonstrated high EQE values of over 10% and obtained EL spectra resembling their emission spectra in solution, confirming the fact that the EL spectra are generated exclusively from the emitters themselves. Pt-14 can be used as an efficient phosphorescent emitter to fabricate a “blue–green” emitting OLED with a maximum EQE of over 18% and CIE coordinates of (0.16,0.36). The CIE coordinates of Pt-16 device are (0.16,0.15), making Pt-16 a perfect candidate as a deep blue phosphorescent emitter. Moreover, it is worth mentioning that 26mCPy, a carbazole-based host material with an estimated triplet energy of 2.9 eV [11a], [13], can be used for deep blue phosphorescent OLEDs if the emitter is judiciously designed. On the other hand, although Pt-15 has a higher emission energy than Pt-16 and can provide an EL spectrum with more desirable CIE coordinates, the Pt-15 device has a maximum EQE of less than 1%. The EL spectrum is broader than the PL spectrum of doped thin film, indicating that the EL spectrum is not generated exclusively from the emitter itself, resulting in a decrease in device efficiency. Thus, the extremely low efficiency of the Pt-15 device

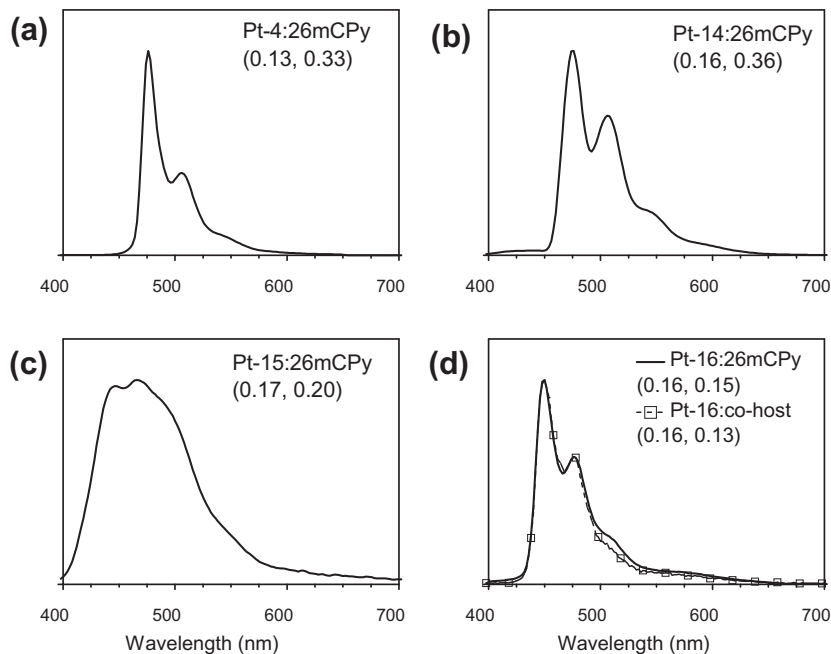


Fig. 4. Normalized electroluminescent spectra, accompanied by CIE values of (a) Pt-4, (b) Pt-14, (c) Pt-15 and (d) Pt-16 devices at 1 mA/cm². The general device structure is ITO/PEDOT:PSS/NPD(30 nm)/TAPC(10 nm)/2% emitter: host(25 nm)/PO15(40 nm)/LiF/Al. The host materials could be either 26mCPy or co-host of TAPC:PO15 (1:1).

Table 1

A summary of device characteristics for the structure: ITO/NPD(30 nm)/TAPC(10 nm)/EML(25 nm)/PO15(40 nm)/LiF/Al. Each device is listed by its emissive layer at a luminance of 100 cd/m². Parameters listed are driving voltage (bias), current density, forward viewing external quantum efficiency (EQE), CIE coordinates and power efficiency (P.E.).

Emissive layer	Bias (V)	Current density (mA/cm ²)	EQE (%)	CIE _x	CIE _y	P.E. (lm/W)
2% Pt-4:26mCPy	5.1	0.35	15.9	0.13	0.33	17.4
2% Pt-14:26mCPy	5.2	0.24	18.1	0.16	0.36	23.3
2% Pt-15:26mCPy	7.8	25.7	0.68	0.17	0.20	0.16
2% Pt-16:26mCPy	4.5	0.81	10.1	0.16	0.15	8.96
2% Pt-16:co-host	3.0	0.51	14.8	0.16	0.13	19.3

can possibly be attributed to the combined results of its low emission efficiency and the use of host materials without high enough triplet energy. Further studies suggest that the utilization of ultra-high bandgap host materials like UGH2 [14] failed to significantly improve the efficiency of the Pt-15 devices.

In order to improve the performance of the Pt-16 devices, a co-host system was utilized to further resolve any potential charge carrier imbalance in the emissive layer. A mixed layer of TAPC:PO15 is documented as one example [12], which can replace 26mCPy as host materials in a similar device setting. Forward viewing external quantum efficiency vs. luminance and current density vs. voltage (inset) are plotted for the device of ITO/PEDOT:PSS/NPD(30 nm)/TAPC(10 nm)/2% Pt-16:TAPC:PO15(25 nm)/PO15(40 nm)/LiF/Al in Fig. 5. A maximum forward viewing EQE of 15.7% was achieved at a current density of $J = 0.02$ mA/cm², and only decreases to a half of its peak value at a current density of $J = 10.9$ mA/cm². This device also gives a maximum forward power efficiency of 22 lm/W and remains at a high 19.3 lm/W at a practical luminance (100 cd/m²). Moreover, the co-host system modified solubility, and thus the molecular packing, of Pt-16 in the emissive layer, resulting in a significant decrease in excimer and aggregate formation and attenuated vibronic features of Pt-16 emission bands (Fig. 4). Such small changes in the EL spectrum yielded highly desirable CIE coordinates of

(0.16,0.13) for the Pt-16 devices, which also demonstrated an independence of current density. The color quality of the Pt-16 device is comparable or even superior to the best deep blue phosphorescent OLEDs in literature which focused on the use of Ir-based complexes [6a]. Although the maximum EQE of the Pt-16 device is lower than that of the Ir(dbfmi) device, the Pt-16 device can maintain an EQE of 14.8% at 100 cd/m² and an EQE of 8.3% 1000 cd/m² due to a small roll-off at a high current density. On the other hand, the EQEs of the Ir(dbfmi) device are 13.3% at 100 cd/m² and 6.2% at 1000 cd/m² [6a].

4. Conclusions

We demonstrated that a series of blue-emitting Pt(N^{^C^N})Cl complexes were developed by engineering the LUMO energy levels of Pt complexes. We have fabricated a deep blue OLED utilizing Pt-16 with a maximum EQE of 15.7% and CIE coordinates of (0.16,0.13). Compared with their Ir-based analogs, Pt(N^{^C^N})Cl complexes can display a “deeper blue” color with similar emission energy due to their narrower emission bandwidth and attenuated vibronic features of their emission spectra. It is also very encouraging to demonstrate that carbazole-based host materials can be used as host materials for efficient deep blue phosphorescent OLEDs. Moreover, Pt-16 is a fluorine-free blue phosphorescent emitter indicating that its design is aligned with molecules that have demonstrated stability for long operational lifetime [15]. Continued characterization and development should provide a viable route to develop stable and efficient deep blue phosphorescent emitters for displays and lighting applications.

Acknowledgements

The authors thank the National Science Foundation (CHE-0748867), the Department of Energy (DE-EE0005075), and Flexible Display Center for partial support of this work. J. L. wants to thank Dr. Asanga Padmameruma and his group from Pacific Northeastern National Lab for providing PO15 material.

References

- [1] (a) S.R. Forrest, Nature 428 (2004) 911;
(b) L. Xiao, Z. Chen, B. Qu, J. Luo, S. Kong, Q. Gong, J. Kido, Adv. Mater. 23 (2011) 926;
(c) M.C. Gather, A. Kohnen, K. Meerholz, Adv. Mater. 23 (2011) 233–2105.
- [2] (a) M.A. Baldo, D.F. O'Brien, Y. You, A. Shoustikov, S. Sibley, M.E. Thompson, S.R. Forrest, Nature 395 (1998) 151;

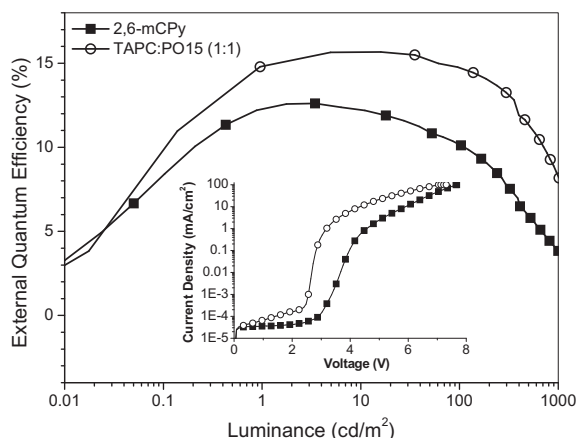


Fig. 5. External quantum efficiency–luminance and current density–voltage (inset) characteristics for the Pt-16 devices with different host materials: 26mCPy and co-host of TAPC:PO15 (1:1). The general device structure is ITO/PEDOT:PSS/NPD(30 nm)/TAPC(10 nm)/2% Pt-16:co-host(25 nm)/PO15(40 nm)/LiF/Al.

- (b) M.A. Baldo, S. Lamansky, P.E. Burrows, M.E. Thompson, S.R. Forrest, *Appl. Phys. Lett.* 75 (1999) 4.
- [3] (a) S. Lamansky, P. Djurovich, D. Murphy, F.A. Razzaq, H.-E. Lee, C. Adachi, P.E. Burrows, S. Forrest, M.E. Thompson, *J. Am. Chem. Soc.* 123 (2001) 4304;
- (b) A. Tsuboyama, H. Iwawaki, M. Furugori, T. Mukaide, J. Kamatani, S. Gawa, T. Moriyama, S. Miura, T. Takiguchi, S. Okada, M. Hoshino, K. Ueno, *J. Am. Chem. Soc.* 125 (2003) 12971;
- (c) X.H. Yang, D. Neher, D. Hertel, T.K. Däubler, *Adv. Mater.* 16 (2004) 161;
- (d) Y.J. Su, H.L. Huang, C.L. Li, C.H. Chien, Y.T. Tao, P.T. Chou, S. Datta, R.S. Liu, *Adv. Mater.* 15 (2003) 884;
- (e) F.I. Wu, H.J. Su, C.F. Shu, L.Y. Luo, W.G. Diau, C.H. Cheng, J.P. Duan, G.H. Lee, *J. Mater. Chem.* 15 (2005) 1035;
- (f) F.I. Wu, P.I. Shih, Y.H. Tseng, G.Y. Chen, C.H. Chien, C.F. Shu, Y.L. Tung, Y. Chi, A.K.Y. Jen, *J. Phys. Chem. B* 109 (2005) 14000;
- (g) M.C. Gather, A. Kohnen, K. Meerholz, *Adv. Mater.* 23 (2011) 233;
- (h) L. Duan, J. Qiao, Y.D. Sun, Y. Qiu, *Adv. Mater.* 23 (2011) 1137.
- [4] (a) C. Adachi, R.C. Kwong, P. Djurovich, V. Adamovich, M.A. Baldo, M.E. Thompson, S.R. Forrest, *Appl. Phys. Lett.* 79 (2001) 2082;
- (b) J. Li, P.I. Djurovich, B.D. Alleyne, M. Yousufuddin, N.N. Ho, J.C. Thomas, J.C. Peters, R. Bau, M.E. Thompson, *Inorg. Chem.* 44 (2005) 1713;
- (c) R.J. Holmes, B.W. D'Andrade, S.R. Forrest, X. Ren, J. Li, M.E. Thompson, *Appl. Phys. Lett.* 83 (2003) 3818;
- (d) S.J. Yeh, M.F. Wu, C.T. Chen, Y.H. Song, Y. Chi, M.H. Ho, S.F. Hsu, C.H. Chen, *Adv. Mat.* 17 (2005) 285;
- (e) S. Tokito, T. Iijima, Y. Suzuri, H. Kita, T. Tsuzuki, F. Sato, *Appl. Phys. Lett.* 83 (2003) 569;
- (f) T. Sajoto, P.I. Djurovich, A. Tamayo, M. Yousufuddin, R. Bau, M.E. Thompson, R.J. Holmes, S.R. Forrest, *Inorg. Chem.* 44 (2005) 7992;
- (g) C.-H. Lin, Y.-Y. Chang, J.-Y. Hung, C.-Y. Lin, Y. Chi, M.-W. Chung, C.-L. Lin, P.-T. Chou, G.-H. Lee, C.-H. Chang, W.-C. Lin, *Angew. Chem. Int. Ed.* 50 (2011) 3182.
- [5] (a) J. Brooks, Y. Babayan, S. Lamansky, P.I. Djurovich, I. Tsyba, R. Bau, M.E. Thompson, *Inorg. Chem.* 41 (2002) 3055;
- (b) B.W. D'Andrade, J. Brooks, V. Adamovich, M.E. Thompson, S.R. Forrest, *Adv. Mater.* 14 (2005) 1032;
- (c) B.W. D'Andrade, S.R. Forrest, *J. Appl. Phys.* 94 (2003) 3101;
- (d) B.W. Ma, P.I. Djurovich, S. Garon, B. Alleyne, M.E. Thompson, *Adv. Func. Mater.* 16 (2006) 2438.
- [6] (a) H. Sasabe, J.-I. Takamatsu, T. Motoyama, S. Watanabe, G. Wagenblast, N. Langer, O. Molt, E. Fuchs, C. Lennartz, J. Kido, *Adv. Mater.* 22 (2010) 5003;
- (b) R.J. Holmes, S.R. Forrest, T. Sajoto, A. Tamayo, P.I. Djurovich, M.E. Thompson, J. Brooks, Y.-J. Tung, B.W. D'Andrade, M.S. Weaver, R.C. Kwong, J.J. Brown, *Appl. Phys. Lett.* 87 (2005) 243507;
- (c) S. Haneder, E. DaComo, J. Feldmann, J.M. Lupton, C. Lennartz, P. Erk, E. Fuchs, O. Molt, I. Munster, C. Schildknecht, G. Wagenblast, *Adv. Mater.* 20 (2008) 3325.
- [7] (a) S.O. Jeon, S.E. Jang, H.S. Son, J.Y. Lee, *Adv. Mater.* 23 (2011) 1436;
- (b) S.O. Jeon, K.S. Yook, C.W. Joo, J.Y. Lee, *Adv. Mater.* 22 (2010) 1872.
- [8] (a) Z. Wang, E. Turner, V. Mahoney, S. Madakuni, T. Groy, J. Li, *Inorg. Chem.* 49 (2010) 11276;
- (b) A.F. Rausch, L. Murphy, J.A.G. Williams, H. Yersin, *Inorg. Chem.* 48 (2009) 11407.
- [9] X. Yang, Z. Xing, S. Madakuni, J. Li, G.E. Jabbour, *Adv. Mater.* 20 (2008) 2405.
- [10] Y. Unger, D. Meyer, O. Molt, C. Schildknecht, I. Münster, G. Wagenblast, T. Strassner, *Angew. Chem. Int. Ed.* 49 (2010) 10214.
- [11] (a) T. Sajoto, P.I. Djurovich, A.B. Tamayo, J. Oxgaard, W.A. Goddard, M.E. Thompson, *J. Am. Chem. Soc.* 131 (2009) 9813;
- (b) S. Develay, O. Blackburn, A.L. Thompson, J.A.G. Williams, *Inorg. Chem.* 47 (2008) 11129.
- [12] (a) V. Adamovich, J. Brooks, A. Tamayo, A.M. Alexander, P.I. Djurovich, B.W. D'Andrade, C. Adachi, S.R. Forrest, M.E. Thompson, *New J. Chem.* 26 (2002) 1171;
- (b) E.L. Williams, K. Haavisto, J. Li, G.E. Jabbour, *Adv. Mater.* 19 (2007) 197.
- [13] N. Chopra, J.S. Swensen, E. Polikarpov, L. Cosimbescu, F. So, A.B. Padmaperuma, *Appl. Phys. Lett.* 97 (2010) 033304.
- [14] X. Ren, J. Li, R.J. Holmes, P.I. Djurovich, S.R. Forrest, M.E. Thompson, *Chem. Mater.* 16 (2004) 4743.
- [15] N.C. Giebink, B.W.D. Andrade, M.S. Weaver, P.B. Mackenzie, J.J. Brown, M.E. Thompson, S.R. Forrest, *J. Appl. Phys.* 103 (2008) 044501.